Soft Matter

Accepted Manuscript

ROYAL SOCIETY OF CHEMISTRY

www.rsc.org/softmatter

Soft Matter

RSCPublishing

ARTICLE

Thermotropical dynamical processes in multiphase polymer systems by (cryo-)AFM

Cite this: DOI: 10.1039/xoxxoooooox

N.B. Matsko[1] and V. Mittal[2],

Received ooth January 2014,
Accepted ooth January 2014

DOI: 10.1039/xoxxoooooox

www.rsc.org/

The structural (volume and enthalpy) relaxation of polymers during physical aging has a great relevance in material science and engineering as it significantly changes the long-term material performance. In this article, we propose methodological approach of (cryo-) atomic force microscopy (AFM) monitoring of macromolecular rearrangements which accompany structural relaxation within bulk of the polymer during physical aging. In contrast to conventional spectroscopic, scattering and thermal analysis techniques, high resolution topographical/phase imaging of the bulk cross-section over a large period of time and within wide range of temperatures (–120°C to +20°C) yields unique information about the evolution of the polymer ultrastructure as a function of time and temperature *in-situ*.

1. Introduction

A thermodynamic system brought out of equilibrium spontaneously evolves to re-establish its equilibrium state. Among the numerous phenomena in nature where such evolution can be observed, of particular interest both from a fundamental and applied point of view is the spontaneous relaxation of glassy materials towards the thermodynamic stable state. This phenomenon is especially relevant for amorphous or semicrystalline polymers, which represent a significant class of glass-forming materials [1-6]. If a glass-forming material is quickly cooled below the glass transition temperature (T_g), its structure departs from the equilibrium as a result of the decreasing molecular mobility, since the molecules are not able to reach their equilibrium conformations in the time scale of the cooling [7]. This may change the crystal structure, degree of crystallinity, perfection of the crystals, orientation of both crystalline and amorphous phases, structural morphology, number of tie chains between the crystallites and as a consequence the entire phase volume [5-8]. However, the non-equilibrium state tends to relax below the glass transition temperature approaching the corresponding stable state with time. This time dependant structural change towards equilibrium, known as physical aging or structural relaxation, is accompanied with measurable property changes [5, 7-11]. This is clearly of technological and engineering significance for thermoplastics, which are commonly melt processed by techniques such as injection moulding and extrusion. These processing methods involve quenching or fast cooling of the polymer from high (melt) temperature to low (typically ambient) temperatures, thus resulting in thermal history, which initiates the process of aging. Products processed in this way, therefore, can be anticipated to age at their service temperatures, involving a time-dependent change in properties such as dimensions, density, modulus, compliance, refractive index and dielectric constant [5]. The macromolecular rearrangements which are related to structural relaxation during physical aging are most commonly analyzed using spectroscopic, scattering and thermal techniques which are based on averaging of the parameters (volume recovery, mechanical compliance, creep shift, etc.) from the entire polymer bulk [12-20]. Therefore, in two chemically identical compositions different values may arise [20]. The clue lies in the recognition that the values of volume recovery and mechanical characteristics are specific for each polymer system (e.g. depending on temperature history, relaxation kinetic, and instantaneous structure of the material) including interphase layers within polymer blend bulk. Here, we propose an alternative method to monitor the evolution of the volume recovery and molecular scale rearrangements, which take place during physical aging. The technique is based on the phenomenon that the polymer block face exhibits a topographical profile after sectioning, which is related to a volume contraction/expansion of each polymer phase including interphase layers present on the block phase surface [21-23]. This is a consequence of the fact that the volumetric changes of each polymer phase (which forms during processing procedures) create a complex tension network within the polymer bulk [5,6].

Therefore, by splitting the polymer bulk by sectioning, it is possible to partially release the tension at least on the block face surface as the constraining surroundings are removed (Fig. 1).

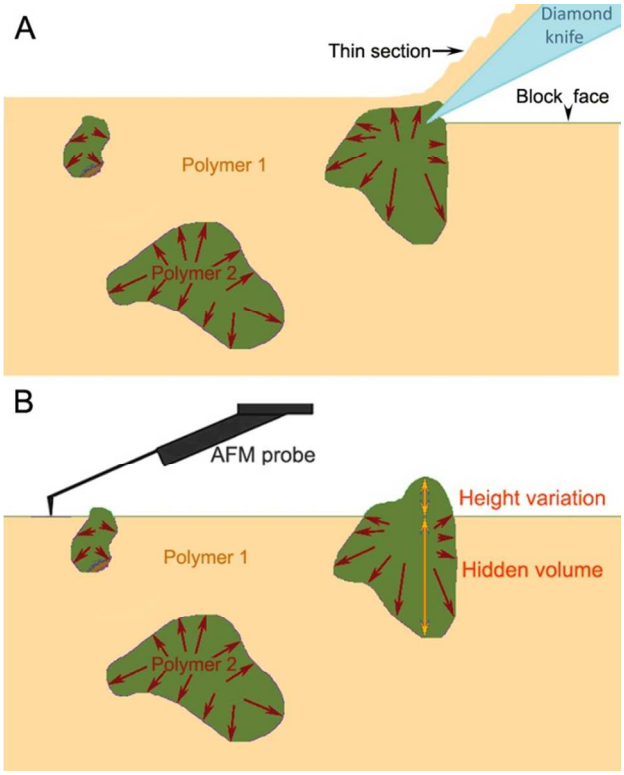

Figure 1. Schematic description of the sectioning - (cryo-) AFM monitoring methodology. (A) Preparation of a block face by ultramicrotomy. (B) AFM analysis of the block face surface.

Subsequently, the topographical profile of the block phase after ultramicrotomy can be detected with high resolution by AFM [24]. As AFM is a high resolution non-destructive surface characterization technique for analyzing soft matter, information about the location, architecture and mechanical properties of macromolecules or polymer chains can be obtained directly from the surface of the unstained and artifact-free block face even at low temperatures [21-26]. Although AFM has been proven to be particularly useful for the investigation of both local macromolecular rearrangements that occur within a singular polymer phase and the entire structural organization of complex polymer systems in general [27, 28], till now this technique has never been used to monitor the evolution of the volume recovery and molecular scale rearrangements, which take place during physical aging.

In this article, we describe an AFM based analytical approach which allows detecting time/temperature dependant structural changes which accompany physical aging phenomenon in complex polymer systems. Following test samples were chosen: polylactid (PLA), polycaprolactone (PCL) and ternary blend of these with thermoplastic starch (PLA-PCL-TPS); binary blend of polyamide-6 and styrene-acrylonitrile (PA6-SAN) and nitrile butadiene rubber (NBR), due to their use in a variety of biomedical and engineering applications. The time dependent structural changes are accompanied with 1) the effect of phase separation between different polymer phases that becomes more pronounced with time and; 2) the glass densification (e.g. permanent increase in density) followed by complete rearrangement of polycrystalline order (e.g. changes in shape and size of polymer nanofibers) for those polymer phases which have utmost topographical contrast just after the production. Besides the morphological appearance, AFM provides information about the volumetric expansion/contraction of each polymer phase which to some degree is related to the hidden phase volume in the depth of the polymer block. Cryo AFM study of elastomers in the temperature regime close to T_g of the polymer also allows one to identify compositional variation such as degree of miscibility (for polymer blends), impurities, polymer phase distributions and the local variation in T_g.

2. Experimental

2.1. Materials

PA6-SAN (70%/30%) was prepared as described earlier by Sailer and Handge [29]. PCL with a trade name of CAPA 6506S was procured from Perstorp Polyols, USA. It had M_w of 50,000 g/mol, T_g of about -60□C and peak melting temperature (T_m) of 60□C (supplier information). PLA procured from Biomer, Germany had a density of 1.25 g/cm^3, T_g 55□C and T_m of 168□C. TPS was based on Hylon VII, which is an unmodified corn starch from National Starch (New Jersey, USA) with an amylose content of 70%. The composition of extruded TPS was 69% of dry starch, 12% of water and 19% of glycerol. PLA-PCL-TPS (50%/40%/10%), PLA-PCL(50%/50%) as well as pure PCL and PLA were processed using mini twin conical screw extruder (MiniLab HAAKE Rheomex CTW5, Germany). A mixing temperature of 160°C for 10 minutes at 80 rpm with batch size of 5 g was used. The screw length and screw diameter were 109.5 mm and 5/14 mm conical respectively. Nitrile butadiene rubber (NBR) latex test sample was taken from commercially available NBR gloves (T_g -73°C (supplier information)), and was embedded in Araldite–Epon embedding mixture, followed by polymerization at 50°C for 72 h.

2.2. Characterization methods

The AFM measurements have been performed using cryo atomic force microscope system SNOTRA [30] over a wide range of temperatures (−120°C to +20°C) and conventional Dimension 3100 AFM/SPM (Veeco, USA) atomic force microscope at ambient conditions. The cryo-AFM system used chemically etched tungsten tips attached to a quartz tuning fork as an AFM probe [31]. A specially designed cryo-AFM was mounted directly within the cryogenic chamber of an ultramicrotome. The cryo-AFM unit moved together with the arm of the cryo-ultramicrotome. The probe approached the surface by a stepper motor when the arm was driven to the upper position. After measurement, the probe was removed

from the sample surface using the same stepper motor. Thereafter, it was possible to proceed with the next section of the sample at the same temperature or adjust other temperature regime by the thermoregulatory system of the cryo chamber [30]. Polymer samples were frozen directly in the cryo-chamber of the instrument.

For the conventional AFM analysis, the polymer samples were mounted in special holders which at the same time fit in the microtome and were suitable for the examination of the block face by atomic force microscopy and light microscopy. Block faces of the composite samples were obtained using a Leica Ultracut E microtome (Leica, Austria) equipped with a diamond knife (Diatome, Switzerland) at −50°C (for PCL, PLA and PLA-PCL-TPS blend), −80°C (for PA6-SAN), and −120 °C (for NBR latex sample). Since the T_g for each polymer phase in above mentioned blends significantly differs from each other, the optimal sectioning temperature has been chosen empirically taking into account two main conditions: (i) the produced block face didn't contain the compression patterns, and (ii) the fracturing of any polymer phases has been avoided.

The block faces of specimens after cryo-ultramicrotomy were slowly warmed up and immediately investigated at room temperature (+20°C). Since long storage of the samples may have influence on the surface morphology of the block faces (e.g. oxidation, light induced changes, etc.), the AFM images have been collected only from freshly prepared cross-sections of non - treated sample blocks with the appropriate age. AFM images were collected in tapping mode using silicon nitride cantilevers with natural frequencies in the 300-kHz range (force constant 20 N/m and tip radius 10 nm (NT-MDT, Russia)). In order to exclude the influence of the AFM measurement condition on the surface topography, the hard tapping regime should be avoided [25]. AFM image processing was performed using Nanoscope v720 software (Veeco, USA). Light microscopy analysis was performed using ZEISS Axioplan light microscope (ZEISS, Germany) equipped with ZEISS Axio Cam ICc 1 CCD camera in reflected polarized light.

Calorimetric properties of the injection moulded blend (both initial (shortly after the production) and aged (270 days after the production)) were recorded on a Netzsch DSC under nitrogen atmosphere. The first-heating scans were obtained from 50 to 250°C using heating rate of 15°C/min. The heat enthalpies used to calculate the extent of crystallinity were recorded in a narrow error range (±0.1%), which were also confirmed by repeated runs.

3. Results and discussion

3.1. The description of the methodology

Physical aging has been observed in a very broad range of polymeric materials including thermoplastic and thermoset matrix composites, liquid crystalline polymers, etc. These particular polymer systems are not specifically subjected for investigation in this article, rather, we examine the aging in

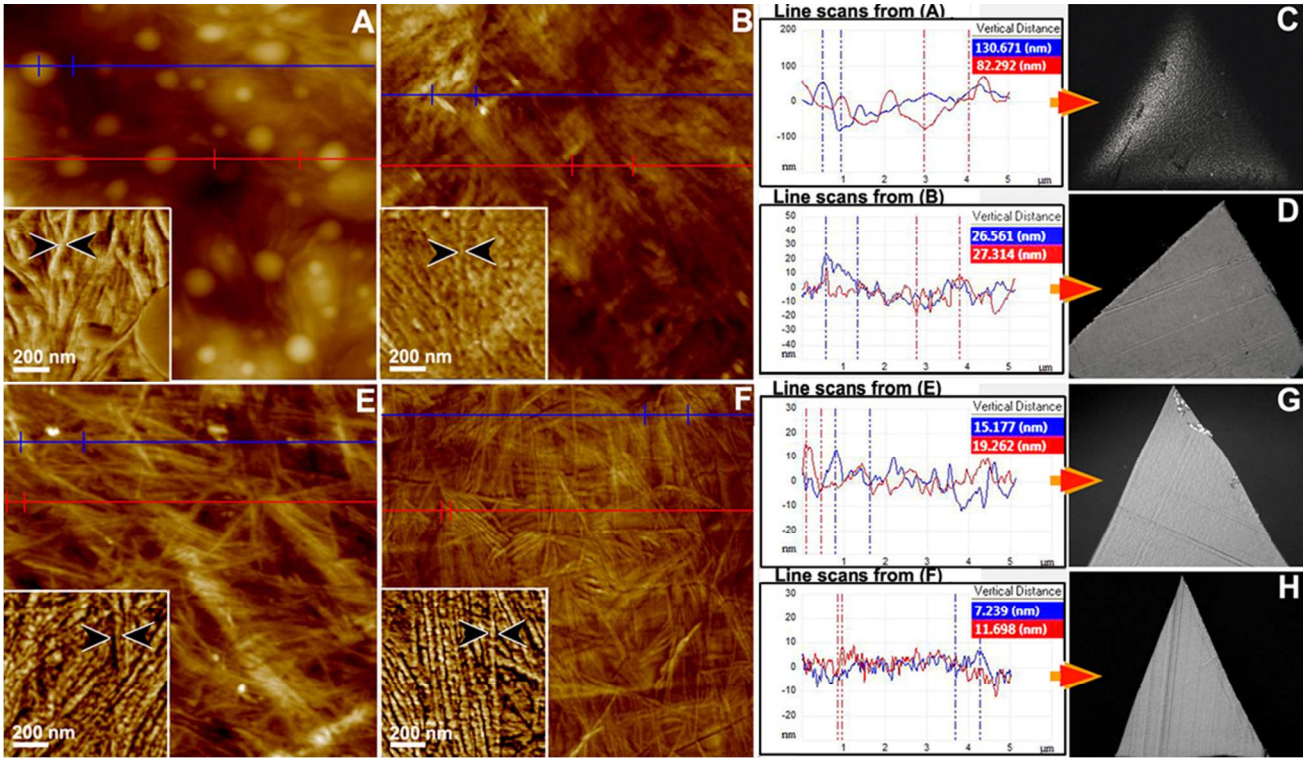

Figure 2. Evolution of volumetric expansion/contraction of PCL (A-D) and PLA (E-H) as a function of time. (A, C, and E ,G) initial state of the samples (14 days after production), (B, D and F, H) aged stage of the samples (270 days after production). Graphical data of two random scan lines (red and blue) for each scan (A, B, E, F) are presented. Vertical dash lines in the line scans plot corresponding to the tick marks in A, B, E, F colour lines. Room temperature light microscopy (C, D, G, H) of freshly prepared cross-sections of the corresponding sample blocks with the appropriate age.

semi-crystalline and amorphous polymers, for which a number of typical AFM detectable effects have been observed.

Figure 2 demonstrates the time dependent structural changes within bulk of pure PCL and PLA polymers. There are two main AFM measurable parameters, which define the difference between initial (14 days after the production) and aged (270 days after the production) polymer morphology. First parameter is a topographical variation of the block face (e.g. the three-dimensional-like quality of the surface). This parameter can be estimated for each particular line scan measurement of the AFM topographical image (Fig. 2 (line scans of A, B and E, F)). Alternatively it can be automatically calculated by AFM software for given area and defines the roughness (e.g. the difference in height between the highest and lowest points on the surface relative to the mean plane). In particular for PCL and PLA, the roughness values in initial state are 205 ± 26.1 nm and 66.1 ± 3.7 nm respectively (for 25 μm^2), and for aged state are 56.2 ± 6 nm and 35,5 ± 2.9 nm respectively (for 25 μm^2).
Physical organisation of macromolecules (e.g. shapes and sizes) is the second microscopically measurable parameter which describes structural relaxation. This factor can be estimated qualitatively by observation the difference between hierarchical organisation of the polymer morphology in initial and aged states. This may include size and shape of the smallest structural units (e.g. macromolecules, crystallites), more general patterns (nanofibers, crystals)), and different polymer phases within complex blends. Quantitative results in this particular case can be useful only for those samples which have ordered structures. In case of PCL and PLA, both qualitative and quantitative results are helpful. As is visible in the Fig. 2 (A, B (inserts)), the diameter of the PCL nanofibers is considerably reduced (in initial state is 63 ± 10.5 nm, in aged state is 40 ± 4 nm). For PLA, the difference between nanofiber diameters in initial state and aged state is not so pronounced (in initial state is 43.8 ± 1.7 nm, in aged state is 32.3 ± 1.9 nm). However, for PCL sample, the fibers morphology is not the only point, which should be considered. As is also obvious from Fig. 2 (A, B), the bundles of nanofibers in initial state are radiated from the centre nucleation site (a spherical phase) forming ring-banded spherulites structure. The spherical phase in aged sample was observed to transform into flat discs. Also, smooth nature of both nanofibers and the spherical phase in initial sample changed to crispy in the aged one. It has to be mentioned that with proper scanning characteristics, the ultrastructure of nanofibers remains unchanged during AFM examination that excludes the influence of the measurement technique on the dynamical process within polymer. Therefore, both of above mentioned AFM parameters can be applied for kinetic study in case of evaluation as function of time (e.g. systematically measured after fixed time period (from days to months)).

From above mentioned results, it is certain that both polymer blocks (PCL and PLA) in the initial state were out of equilibrium. The reduction of the topographical variation in aged samples indicates that the tension within polymer blocks was reduced e.g. volume recovery took place. Simultaneously, modifications in hierarchical nature of the polymer morphology in initial and aged states indicate that macromolecular organisation of both samples was rearranged due to reduction in the diameter of the main structural units of PCL and PLA (e.g. polycrystalline nanofibers).
The differential scanning calorimetry (DSC) measurements of PLA[32], PCL[33] and PLA-PCL blend (Fig. 3) as function of time indicate that the peak melting point of both PCL and PLA has increased in the aged sample. Consequently, area under the melt transitions (which indicates melt enthalpy and crystallinity) increased for both PCL and PLA in the aged samples [32, 33], indicating their enhanced crystallinity with time. Additionally, the PCL/PLA transition (Fig. 3) had area ratio of 1 in the initial sample, whereas it increased to 1.15 in the aged sample indicating that the PCL is more enhanced in crystallinity than PLA in the aged sample. It has been, therefore, revealed that AFM and DSC results are in good agreement since diameters of polycrystalline nanofibers for both PCL and PLA were reduced by 1.6 and 1.4 times correspondingly in the aged sample. This effect can be achieved only by increasing of packing density of nanofibers and thus by increasing of crystallinity of the samples since nanofibers have a polycrystalline nature. Considering the above results of DSC, it can be concluded that proposed AFM based approach provided information which can be easily correlated with conventional technique used for the investigation of structural rearrangements in polymer systems with specific capability of monitoring of morphological transformation during physical aging at each particular point of the cross-section of polymer block with nanometer resolution.

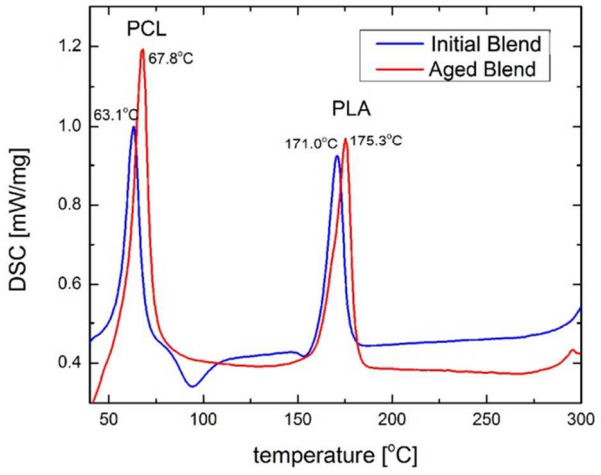

Figure 3. DSC thermograms of PLA-PCL blend measured 14 days after the production (Initial Blend) and 270 days after the production (Aged Blend).

3.2. Physical aging dynamics in complex semicrystalline polymer blends

3.2.1. Effect of separation between different polymer phases

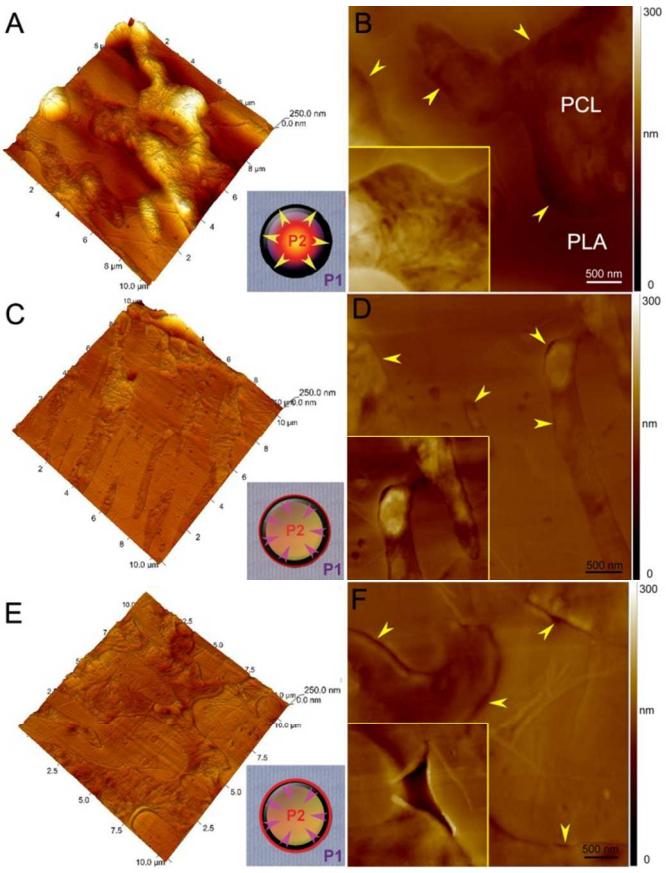

Figure 4. The effect of phase separation between different polymer phases as a function of time for PLA-PCL-TPS blend. Room temperature AFM topographical images of freshly prepared cross-sections of the sample blocks with the appropriate age: (A, B) 14 days after production, (C, D) 60 days after production and (E,F) 180 days after production. Yellow arrows indicate areas of interphase between PCL and PLA. Insets: P1-polymer 1; P2-polymer 2.

Polymer blending is a cost-effective technique to design new materials which combine advantageous properties of different polymers. Usually a polymer blend is a mixture of two or more different species of polymers. From the thermodynamic perspective, the dissolution of polymers into each other is unfavorable due to the low entropy of mixing for high molecular mass materials. Most polymer pairs are therefore immiscible, which leads to a multi-phase morphology [34]. Furthermore, most immiscible polymer compositions suffer from poor interfacial adhesion which causes inferior mechanical properties of solid blends. Due to this, long-term prediction of the interfacial behavior is of utmost importance[35-37]. AFM study of the block phase surface can provide information about long-term behavior of the interfacial adhesion within polymer bulk by monitoring the variation in volumetric expansion/contraction of each particular polymer phase. The blends which exhibit a considerably strong topographical variation between phases most probably will undergo a phase separation process after structural relaxation (Fig. 4). The assumption is organized as follows: usually, the isothermal volume (or length) expansion/contraction of polymer glass is monitored following a temperature above/below the glass transition temperature [5,6]. For those blends, which contain polymers with considerably different temperature dependent properties (T_g, cooperative molecular mobility, volume recovery function), it means that one phase may expand within other one and occupy a higher volume than it can take up in the relaxed state. The effect is particularly pronounced for those blends which have been transformed quickly to a solid state from melt.

Furthermore, during physical aging process leading the glassy state to equilibrium, the ultrastructural densification in uniaxial extension and compression cause the volume contraction of this particular phase. The highest stress in this case is localized within interphase connection regions and sets up the basis for phase separation. As an example, we have chosen academically and commercially relevant biodegradable polymer blend PLA-PCL-TPS [38, 39]. PLA-PCL-TPS blend, as most polymeric blends, is proven to be thermodynamically immiscible, leading to poorly compatible heterogeneous blends having multiphase morphology with poor interfacial adhesion, subsequently impacting the final mechanical properties of the blend [38, 39]. However, the results obtained by proposed AFM based technique demonstrate that the interfacial connection between PCL, TPS and PLA phases exhibits an excellent phase adhesion shortly after the production. As is clearly visible in Fig. 4 (A, B), no phase separated regions can be observed in the sample 14 days after the synthesis of the blend. The topographical variation between PCL and PLA (two main components of the particular blend) phases was observed to be significantly high (in some regions more than 250 nm). In 60 days, the volumetric expansion of PCL phase reduced by a factor of 5, and the first signs of phase separation between PCL and PLA could already be detected (Fig. 4 (C, D)). The topographical contrast between PCL and PLA did not show any further change even after 180 days of blend production indicating that the dynamic polymer bulk approached the corresponding stable state. However, the effect of phase separation became more pronounced with time and can be observed in each interfacial connection regions (Fig. 4 (E, F)). Although term "physical aging" can be accurately applied here only to PLA and TPS phases since T_g of PCL is determined as -60°C (thus, it already exists in the rubbery state at room temperature), the AFM investigation of the initial state of pure PCL (Fig. 2) demonstrates that even at room temperature the bulk of PCL is metastable (i.e. out of equilibrium). The possible explanation for this phenomenon is following: polymeric material, as in the current study, is almost always in metastable state. Most polymeric liquids "freeze in" below T_g. However, T_g does not represent a thermodynamic transition, but a temperature signaling the very rapid rise of viscosity, hence it does not normally feature in phase consideration. This applies on several levels: the glassy solid itself will be metastable because it possesses excess volume, enthalpy etc., even within the liquid phase stability regime. It will become multiply metastable when passing into regimes of other phases, in which it is prevented to transform due to restricted molecular

mobility.[40] This effect is especially pronounced for complex polycrystalline multiphase systems like PLA-PCL-TPS blend.

The non-equilibrium state of each polymer phase within the bulk approaching the corresponding stable state with time leads to volume recovery. However, due to considerably different temperature dependent properties of PCL and PLA, the structural relaxation kinetics of these phases also differs, as concluded from the change in topographical variation of PCL and PLA with time (Fig. 4). Because of immiscibility of the blend, most of the tension is localised in narrow interfacial regions between PCL and PLA. The interfacial macromolecular connections are not able to compensate the stress which leads to phase separation phenomenon with time. Thus, the phase separation between PCL and PLA may results not only due to weak chemical connection between those two phases as suggested in literature, but also is a consequence of structural relaxation taking place during aging history. This is confirmed by the fact that first signs of phase separation between PCL and PLA were detected at very local area of the sample by AFM when the volumetric changes of one polymer phase within bulk took place, but the actual volume occupied by each phase remained the same as the bulk was solidified.

3.2.2. Evolution of ultrastructural organization of polymer phases as a function of time

The time dependent structural change towards equilibrium is accompanied with AFM measurable mechanical property change. Fig. 5 represents AFM phase images of PCL and PLA, where phase shift is related to the hardness and elastic modulus of the materials [25].

There are three factors to be considered: (1) densification of the PCL bulk (e.g. the distance between polymer nanofibers is reduced (Fig. 5 A, D, B, E)); (2) deformation of the PCL ultrastructure 180 days from the production (e.g. the polycrystalline organization of PCL fibers is partially or sometimes completely lost (Fig. 5 C, F)); (3) in contrast, the ultrastructural organization of PLA within polymer bulk did not change much within 180 days of observation.

Important to mention here is that the term "physical aging" [41], as applied to polymers, involves only reversible changes in properties, with no permanent modification on the structure, either chemical or physical, of the material [5]. In case of ternary blend, one can observe both reversible (absence of significant structural modifications of PLA) and irreversible (permanent ultrastructural deformation of PCL) changes. This fact brings to the conclusion that complex polymer systems most probably suffer from more than one superimposed kinetic processes induced by initial metastability of the system and thus cannot be easily interpreted as "physical aging" only. Such changes have to be particularly considered for those applications where nano-fibrous network structure is especially important (e.g. biomedical applications, tissue engineering scaffolds, etc.). In this context, AFM monitoring of the sample morphology can be very useful as it allows to clarify the difference between reversible and irreversible structural changes at the level of individual macromolecule.

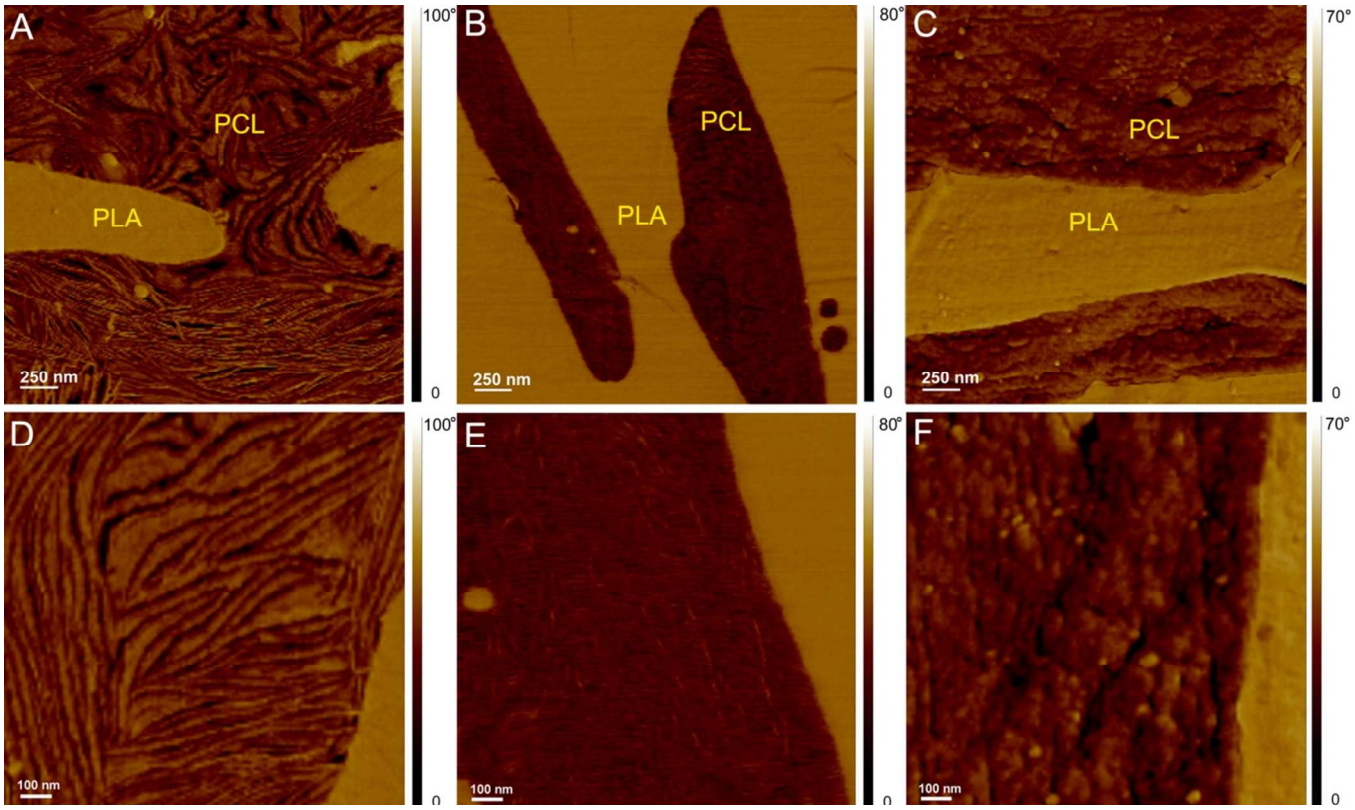

Figure 5. Evolution of ultrastructural organization of polymer phases as a function of time for PLA-PCL-TPS blend. Room temperature AFM phase images of freshly prepared cross-sections of the sample blocks with the appropriate age. (A, D) 14 days after production, (B, E) 60 days after production and(C, F) 180 days after production.

3.2.3. Information about the volumetric expansion/contraction of each polymer phase which to some degree also represents the hidden phase volume in the bulk

As can be seen in Fig. 4 and 5, the PLA-PCL-TPS blend is fully immiscible. The inherent immiscibility and occasionally the large interfacial tension make it difficult to obtain a fine dispersion of the blend components during melt mixing and, under quiescent conditions, it drives phase coarsening phenomena such as coalescence and Oswald ripening [42]. In the latter context, the importance of phase size is emerging as a determining factor not only for the thermodynamic stability *per se* but also for the stability sequence, including the possibility of sequence inversion.

In order to able to get information about phase distribution morphology within a polymer bulk, one would require analytical imaging approach such as 3D reconstruction techniques (tilt-series-based tomography or serial section tomography). Both of these techniques are time consuming and require additional equipment which is not always available. Alternatively, the investigation of the cross-section of polymer blends by AFM shortly after the production (e.g. when the blend itself is metastable because it possesses excess volume, enthalpy, etc.) provides information about phase distribution in both: 2D and 3D. 2D morphology (in terms of physical organization of macromolecules) of the blend can be easily obtained by evaluation of the block face surface of the sample after ultramicrotomy. Besides the morphological appearance, AFM provides also information about the volumetric expansion/contraction of each polymer phase which to some degree is related to the hidden phase volume in the depth of the polymer block. As observed in Fig. 6, the surface roughness of PCL phase (R_a or average deviation) diverges for point 1 (Fig. 6 (C)) and point 2 (Fig. 6 (D)) in the 14 days old metastable blend, in contrast to the 30 days and 180 days old samples where entire block face surface remains relatively homogeneous. The ultimate origin of this phenomenon lies in the fact that within the metastable polymer phase, the mechanical (from the surrounding phase), electrostatic and thermodynamic (due to out-of-equilibrium state of the macromolecules) forces create non-linear tension dispersion which depends on the shape of the metastable phase (e.g. from its volume and spreading area). Consequently, after the partial relaxation of this tension on the block face surface, complex topographical profile is created (Fig. 1). The closer the metastable phase to its equilibrium state, the lower the tension within the volume, and as a consequence, plain topographical profile may be observed. This assumption can also be supported

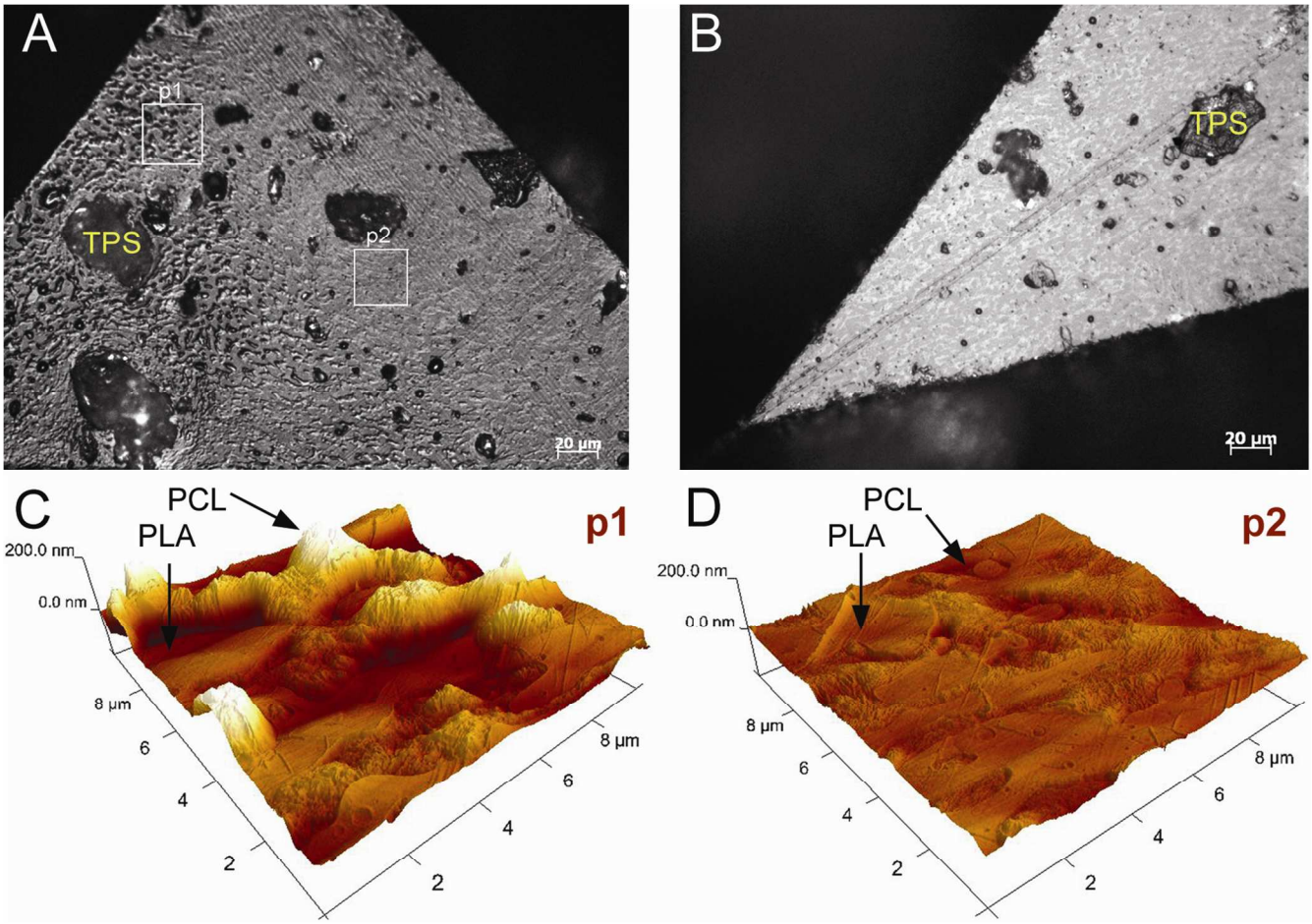

Figure 6. Evolution of volumetric expansion/contraction of polymer phases as a function of time for polylactid-polycaprolactone-thermoplastic starch (PLA-PCL-TPS) blend. Room temperature light microscopy (A, B) and AFM topographical images of freshly prepared cross-sections of the sample blocks with the appropriate age: (A, C, D) polymer samples 14 days after production and (B) polymer sample 120 days after production.

by the fact that pure PCL block after transition through the glass transition temperature (due to the cooling down the polymer block below -60°C exhibits a clear volumetric expansion with maximum magnitude in the block face center (Fig. 2C). Important to mention is that in 180 days, the same sample exhibited no visible topography on freshly prepared block face surface (Fig. 2D). In order to generalize this assumption, the roughness of PA6-SAN polymer blend was measured[29] (a kind gift of Dr. Sailer, ETH Zürich). This test sample has been chosen due to following characteristics: (i) perfectly spherical shape of the PA6 phase which allows to accurately predict the hidden polymer volume from the cross-section diameter and (ii) amorphous nature of SAN phase, which after ultramicrotomy exhibits no topographical features except section artifacts, which have to be taken into account in the quantification analysis.

As shown in Fig. 7 (B), the roughness of the PA phase increased with the diameter of the sphere. Simultaneously, the section artifacts (e.g. compression, knife marks, etc.), which can be estimated from SAN area, also demonstrated an increase in the roughness with the diameter of measured area. However, the entire input from the knife marks and compression of the block face surface was less pronounced than the increase of roughness from the PA6 phase. In order to analyze the effect of temperature history on the modification of the sample ultrastructure (e.g. the detailed structure), the experiments were performed at room temperature and cryo conditions. It was required to clarify whether cooling of the sample below 0°C (which usually occurs in freeze-fracture analysis or cryo-ultramicrotomy) may affect the interfacial connection between two phases of the blend and to estimate the impact of the low temperature transition history on the volumetric change of the PA6 phase. Both of these fundamental aspects have also a methodological relevance. Freeze fracture analysis is very often used as technique for the detection of the efficiency of the chemical compatibilization between phases in polymer blend. However, till now clear understanding about the influence of the method itself on the parameters to be investigated e.g. interfacial connection in this particular case does not exist. Cryo ultramicrotomy, which is a common method to prepare ultrathin sections and block faces of the polymer samples for microscopy, should also be taken into account as factor which may modify the sample ultrastructure (excluding well known section artifacts).[2]

As is visible in the graph in Fig. 7 (C), the roughness of PA6 phase was estimated after sectioning and AFM analysis at room temperature, at cryo condition (-80°C), and consequently after sectioning at low temperature, warming up the sample and measuring once again at room temperature. For the cryo AFM measurements, a newly developed cryo AFM (SNOTRA) has been used [30]. From Fig. 7, it is clear that the roughness of PA6 phase at low temperature remained almost the same (near 40 nm) independently of the diameter of the analyzed area. This data appeared to be logical as the macromolecular movements responsible for the volumetric relaxation of the metastable polymer phase were partially blocked at low temperature. However, after warming up the blend till room temperature, the ultrastructure was not recovered fully and the volumetric expansion of PA6 phase after freezing was much less pronounced than before freezing. The effect was very interesting especially considering that the glass transition temperature of both polymers in the blend were significantly

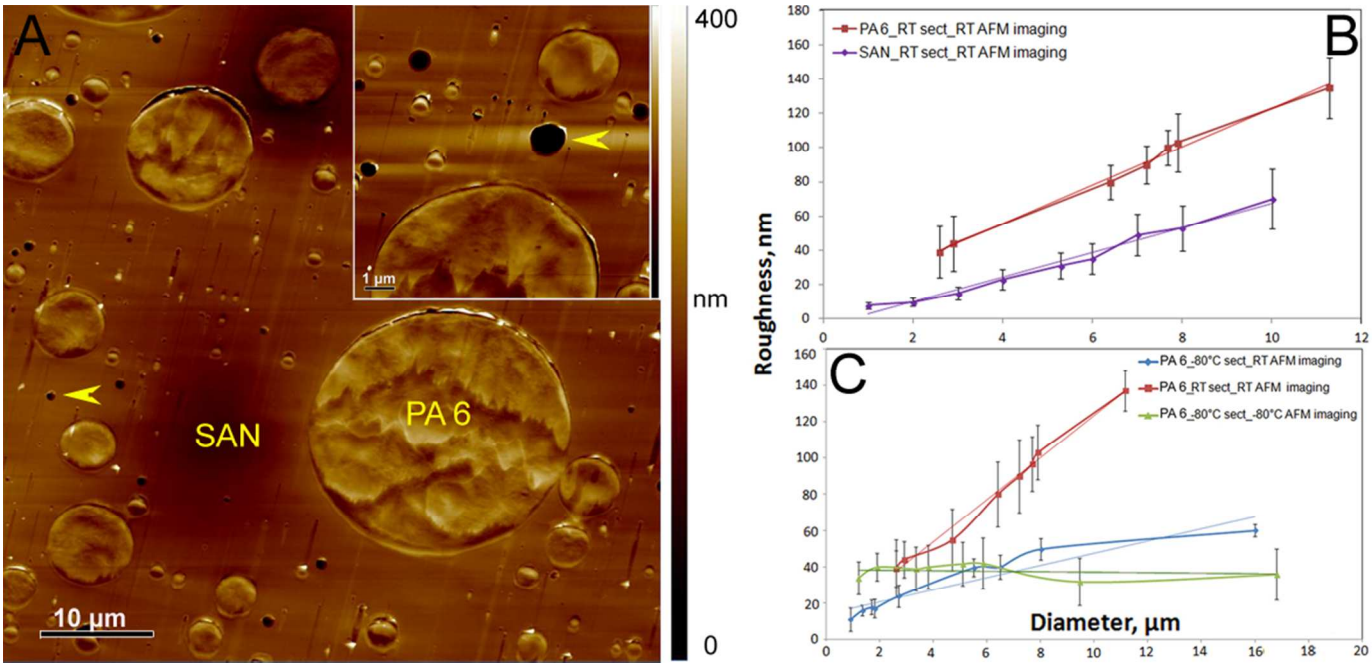

Figure 7. Evolution of volumetric expansion/contraction of each phase of PA6-SAN polymer blend as a function of temperature. (A) Room temperature (RT) AFM topographical image of block which was sectioned at room temperature, (A (insert)) room temperature AFM topographical image of the block which was frozen till -80°C, slowly warmed up and sectioned at room temperature; (B) dependence between roughness and diameter of the PA6 and SAN phases at room temperature and (C) dependence between roughness and diameter of the PA6 phase in accordance with temperature history. The lines are not a curve fit but a visual aid.

above 0°C (T_g PA6 is 53°C, T_g SAN is 109°C) [29]. In other words, during freezing the sample till -80°C, none of the phases experienced transition through the glass transition temperature. Second point to be mentioned here is that after sectioning and examination at room temperature of particularly the same sample which was frozen before, the interfacial connection between PA6 and SAN (Fig. 7 (insert)) was partially disturbed and fracture of the small PA6 droplets as well as numerous gaps between larger PA6 spheres and matrix were detected all over the block face. Thus, the polymer dynamic especially at low temperature conditions appeared to be a very complex phenomenon requiring further investigation in this area. However, it is important to stress that low temperature methods for the sample preparation and analysis of polymer system may change the original ultrastructure of the sample and, therefore, the obtained results may be misleading.

3.2.4. Low temperature real-time monitoring of local glass transition temperature of elastomers in order to map mixing behavior and variation in phase composition at the nanoscale in vivo

A serious limitation of conventional bulk thermal methods like DSC, thermo-mechanical analysis (TMA) and dynamic mechanical analysis (DMA) is that they can only measure a sample-averaged response and cannot offer specific information on localized defects, structural non-uniformities or chemical heterogeneities. In addition, these techniques cannot provide thermal property data of coatings or film surfaces or interfaces that are less than a few microns thick. Transition temperature microscopy (TTM) [43] is a measurement technique of nanoscale thermal analysis (nano-TA) which makes use of a thermal probe to locally heat the surface of a sample while simultaneously monitoring the softening of the sample surface under the heated probe. The nano-TA technique is similar to TMA with the important difference that instead of heating the entire sample, as is done in a TMA experiment, nano-TA probes the thermal response of the material in contact with the probe and therefore can locally determine the transition temperature of the sample on the micro or nanoscale. However, this technique has a severe limitation as it is effective only for materials which have glass transition temperature above room temperature. Therefore, almost all type of elastomers (thermosets and thermoplastic elastomer) and there composites as well as a vast majority of other soft polymer materials (e.g. hydrated) having glass transition temperature below 0°C cannot be sufficiently characterized by TTM in terms of high resolution structural-thermal organization. As an alternative, a real-time monitoring of the low temperature thermotropical dynamical processes such as volumetric relaxations near the glass transition temperature can be performed using cryo-AFM (SNOTRA)[30]. This technique provides an opportunity to observe the evolution of the sample ultrastructure as a function of temperature (from −120°C to +50 °C) *in-situ* and maps mixing behavior and variation in phase composition at the nanoscale. Fig. 8 represents a correlative study of nitrile-butadiene latex material by transmission electron microscopy (TEM) and AFM at room temperature and cryo conditions. It has to be mentioned here that the wide range of the products which include synthetic rubbers are generally produced by emulsion polymerization [44]. A typical emulsion polymerization formulation comprises four basic ingredients: 1) monomer, 2) dispersion medium, 3) emulsifier and 4) initiator. Emulsifier and initiator are usually localized mostly on the surface of the latex spheres. (See Fig. SI 1). Obviously, it can be expected that

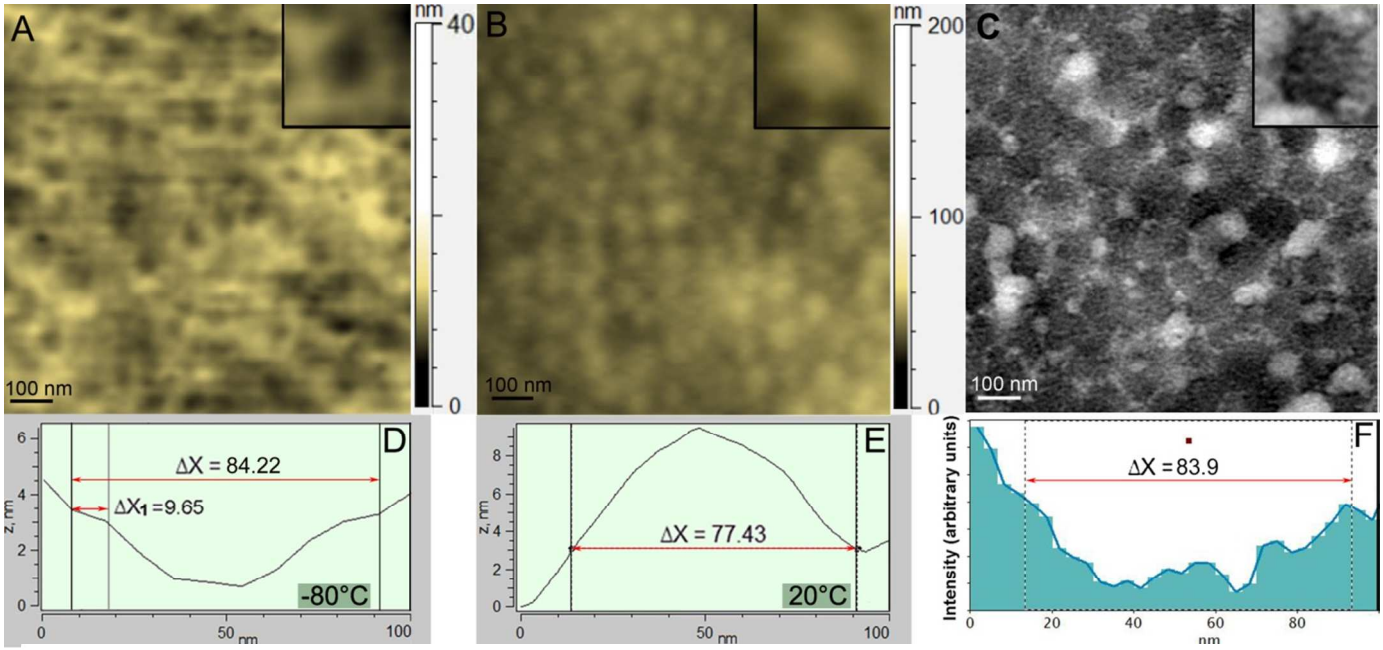

Figure 8. Ultrastructural relaxation of NBR as function of temperature. (A) Low temperature (-80°C) AFM topographical image of cryo (-80°C) sectioned sample, (B) RT AFM topographical image of cryo sectioned and slowly warmed up sample, (C) bright field TEM micrograph of ultrathin (near 50 nm) non-stained section of the particularly the same NBR block, (D, E) topographical and (F) intensity profiles of the selected (inserts) latex spheres.

the surface layer will have different mechanical and thermal properties since the local glass transition temperature should be slightly different for pure polymer and its mixture with other components. However, TEM micrographs did not emphasize any difference between central part of the latex spheres and their edge (due to projection issue) (Fig. 8 (C, F)). The observation of the same material by AFM (low temperature sectioning followed by room temperature observation) did not highlight the difference between central and edge parts either. However, *in vivo* AFM study at the temperature which is close to T_g of NBR (from -70°C to -90°C) clearly indicated the difference between central part of the spheres and their surface layer. Topographical profile of the selected particle (Fig. 5 (D)) shows that the edge layer was about 10 nm wide. Important to mention here is that the topographical variation became more pronounced between sides and central areas of latex spheres when the temperature of sectioning and AFM measurement was kept between -80°C and -70°C. With deliberately increasing the temperature, the central area volumetrically expanded and the topographical contrast between edge and central parts disappeared completely (Fig. 8 (B)).

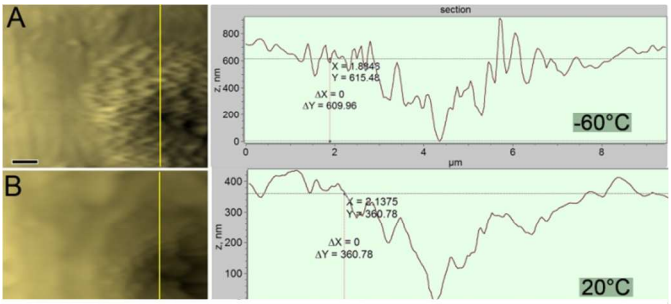

Figure 9. Ultrastructural relaxation of polylactid-polycaprolactone (PLA-PCL) as function of temperature. (A) Low temperature (-60°C) AFM topographical image of cryo (-60°C) sectioned sample, (B) RT AFM topographical image of the same area of sample after it was slowly warmed up with corresponded topographical profiles. Scale bars 1µm.

Such behavior (e.g. the rearrangement of polymer ultrastructure at room temperature) is common for most soft polymers (see Fig. 9) and has to be particularly considered for those applications where accurate dimensional characteristics are required. It is important to emphasize that the structural evolution in the aging regime in short time scale (from seconds to minutes) [5,6] was strongly influenced by the temperature fluctuations within cryo-chamber during heating procedure. Due to the superimposition of the dynamic processes, the interpretation of the images became complex thus requiring additional investigation. However, cryo AFM study of elastomers in the temperature regime which is close to T_g of the entire polymer block allows one to identify compositional variation such as degree of miscibility (for polymer blends), impurities, polymer phase distributions and the local variation in T_g. In most applications, a reliable understanding and control over above mentioned parameters can significantly enhance the scientific understanding of the fundamental phenomena.

Conclusions

The novel (cryo-) AFM based analytical approach proposed in this article represents a powerful asset towards substantial structural characterization of dynamical processes which take place in the bulk of amorphous/polycrystalline multiphase polymer systems during physical aging. In particular, this involves the evolution of the volume recovery, molecular scale rearrangements and thermotropical processes near T_g which can be observed *in-situ* with high resolution. The technique is based on the phenomenon that stresses within a polymer bulk arising due to transition through T_g of each polymer phase of sample (during production or sample preparation procedure) can be partially released on the block face surface immediately after cross-sectioning of the polymer bulk. (Cryo-) AFM analysis performed immediately after the sectioning procedure in the temperature controlled environment indicated that

1) the effect of phase separation between different polymer phases became more pronounced with time;

2) the densification phenomenon followed by the rearrangement of the polycrystalline structure was evident for those polymer phases which had utmost topographical variation just after the T_g transition and

3) the different polymer phases had independent behavior, exhibiting self-governing (and well defined) glass transitions and individual structural relaxations. (Cryo-) AFM analysis at temperatures close to T_g of the material under investigation allows to identify such compositional variation as degree of miscibility (for polymer blends), impurities, polymer phase distributions and local variation in T_g.

Acknowledgements

The authors are indebted to Anton Efimov and Ferdinand Hofer for fruitful discussions.
Financial support of Austrian Cooperative Research (ACR) is highly appreciated.

Notes and references

[1]Graz Centre for Electron Microscopy, Steyrergasse 17, A-8010 Graz, Austria.
[2]Chemical Engineering Department, The Petroleum Institute, Abu Dhabi, UAE.

Electronic Supplementary Information (ESI) available. See DOI: 10.1039/b000000x/

1 L. C. E. Struik, Physical Aging in Amorphous Glassy Polymers and Other Materials, Elsevier Science, Amsterdam, The Netherlands, 1st edn, 1978.
2 A. J. Kovacs, Fortschr. Hochpolym.-Forsch., 1963, 3, 394–508.
3 G. B. McKenna, Glass Formation and Glassy Behavior, Pergamon Press, Oxford, 1989.
4 I. M. Hodge, Science, 1995, 267, 1945–1947.
5 J. M. Hutchinson, Prog. Polym. Sci., 1995, 20, 703–760.
6 D. Cangialosi, V. M. Boucher, A. Alegría and J. Colmenero, Soft Matter, 2013, 9, 8619-8630.

7 J.P. Fernandez-Blazquez, A. Bello, E. Perez, Polymer Bulletin, 2007, 58, 941-949
8 Encyclopedia Of Polymer Science and Technology, John Wiley and Sons, New York, 4th and, 2014.
9 I. M. Hodge, J. Non-Cryst. Solids, 1994, 169, 211–266.
10 E. Donth, J. Korus, E. Hempel and M. Beiner, Thermochim. Acta, 1997, 305, 239–249.
11 T. Hecksher, N. B. Olsen, K. Niss and J. C. Dyre, J. Chem. Phys., 2010, 133, 174-514.
12 R. Greiner and F. R. Schwarzl, Rheol. Acta, 1984, 23, 378–395.
13 R. WimbergerFriedl and J. G. deBruin, Macromolecules, 1996, 29, 4992–4997.
14 C. G. Robertson and G. L. Wilkes, Macromolecules, 2000, 33, 3954–3955.
15 S. L. Simon, J. W. Sobieski and D. J. Plazek, Polymer, 2001,42, 2555–2567.
16 P. Slobodian, P. Riha, A. Lengalova, J. Hadac, P. Saha and J. Kubat, J. Non-Cryst. Solids, 2004, 344, 148–157.
17 M. Liska and M. Chromcikova, J. Therm. Anal. Calorim., 2005, 81, 125–129.
18 P. Riha, J. Hadac, P. Slobodian, P. Saha, R. W. Rychwalskiand J. Kubat, Polymer, 2007, 48, 7356–7363.
19 J. Malek, R. Svoboda, P. Pustkova and P. Cicmanec, J. Non-Cryst. Solids, 2009, 355, 264–272.
20 S. Spoljaric, A. Genovese, T. K. Goh, A. Blencowe, G. G. Qiao and R. A. Shanks, Macromol. Chem. Phys., 2011, 212, 1677–1691.
20 G. Calleja , A. Jourdan, B. Ameduri, J-P. Habas, European Polymer Journal, 2013, 49, 2214–2222.
21 N. Matsko, Ultramicroscopy, 2007, 107, 95–105.
22 N. Matsko, & M. Mueller, J Struct Biol, 2004, 146, 334–343.
23 V. Mittal, & N.B. Matsko, Analytical Imaging Techniques for Soft Matter Characterization. Heidelberg: Springer. 2012
24 G. Binnig, C. Gerber, E. Stoll, T. R. Albrecht and C. F. Quate, Europhys. Lett., 1987, 3, 1281.
25 S. N. Magonov and D. H. Reneker, Annu. Rev. Mater. Sci., 1997, 27, 175.
26 R. Steinbrecht and K. Zierold, Cryotechniques in Biological Electron Microscopy, Springer-Verlag, New York, USA, 1987.
27 T. Semba, K. Kitagawa, U. S. Ishiaku, and H. J. Hamada. Appl. Polym. Sci., 2006, 101, 1816–1825.
28 Y. Na, Y. He, X. Shuai, Y. Kikkawa, Y. Doi, and Y. Inoue. Biomacromolecules, 2002, 3 (6), 1179-1186.
.29 C Sailer, U.A. Handge, Macromolecules, 2007, 40, 2019-2028.
30 A. Efimov, H. Gnaegi, R. Schaller, W.Grogger, F. Hofer, N. Matsko. Soft Matter, 2012, 8, 9756.
31 N. B. Matsko, J. Wagner, A. Efimov, I. Haynl, S. Mitsche, W. Czapek, B. Matsko, W. Grogger and F. Hofer, J. Mod. Phys., 2011, 2, 72.
32 H. Cai, V. Dave, R. A. Gross, and S. P. McCarthy. J. Polym. Sci. B Polym. Phys., 1996, 34, 2701–2708.
33 A. Campos, J. C. Marconato, and S. M. Martins-Franchetti. Polímeros, 2012, 22(3), 220-227.
34 P.R. Donald , C. B. Bucknall, Polymer Blends Formulation and Performance, John Wiley & Sons, New York, 2000.
35 M. E Broz, D. L. VanderHart, N. R. Washburn, Biomaterials, 2003, 24 (23), 4181−4190.
36 N. López-Rodríguez, A. López-Arraiza, E. Meaurio, J. Sarasua, R. Polym. Eng. Sci. 2006, 46 (9), 1299−1308.
37 C. L.Simões, J. C. Viana, A. M. Cunha, J. Appl. Polym. Sci. 2009, 112 (1), 345−352.
38 P. Sarazin, G. Li, W. J. Orts, B. D. Favis, Polymer, 2008, 49, 599–609.
39 A-L. Goffin, Y. Habibi, J-M. Raquez, and P. Dubois, ACS Appl. Mater. Interfaces, 2012, 4 (7), 3364–3371.
40 A. Keller. Pure & Appl. Chem., 1992, 64(2), 193-204.
41 F. Simon, Z. Anorg. Allg. Chem., 1931, 203, 219–227.
42 B. Crist and A. R. Nesarikar, Macromolecules, 1995, 28, 890.
43 L. T. Germinarto, C. K. Schoff, K. Kjoller, C. Prater, K. Sahagian, JCT CoatingsTech, 2010.
44 R. G. Gilbert, Emulsion Polymerization: a Mechanistic Approach, Academic Press, London, 1996.